*32nd EPS Conference on Plasma Phys. Tarragona, 27 June - 1 July 2005 ECA Vol.**29C**, P-1.007 (2005)*

Fine Structure of Type-I Edge Localized Modes in the Steep Gradient Region in ASDEX Upgrade

B. Kurzan, H. D. Murmann, J. Neuhauser and the ASDEX Upgrade Team

Max-Planck-Institut für Plasmaphysik, EURATOM Association, Boltzmannstr. 2, D-85748 Garching

Introduction

A common feature of Edge Localized Modes (ELMs) is the observation of magnetic field aligned filamentary structures, probably originating from the hot edge pedestal region and moving outward, transporting particles and energy rapidly into the scrape-off layer (SOL) (see [1] and references therein). On ASDEX Upgrade, helical structures have been clearly identified on first wall structures, e.g. by fast 2D-thermography on divertor targets [2] and low field side limiters [3], and in the low field side SOL by Langmuir probes [4, 5]. With the vertical Thomson scattering system on ASDEX Upgrade [6] these results can be complemented by a quantitative analysis of the ELM perturbations in the hot pedestal region near and inside the separatrix. During Type-I ELMs localized maxima and corresponding minima (‘blobs’ and ‘holes’) in the electron density and temperature are clearly visible in the steep gradient region inside the separatrix on 2D-images, obtained in the poloidal plane.

Experimental Setup

The vertical Thomson scattering diagnostic consists of a bundle of up to six vertically launched, radially staggered Nd-YAG laser beams. The whole system can be shifted radially to measure core or, as in the present case, edge plasma profiles and structures. The scattered light is observed from the low-field side in 16 spatial channels with one optical detection system per channel only. The radial resolution is retained by firing the radially staggered lasers one after the other. Altogether, this arrangement forms a vertically stretched (R, z)-matrix of scattering volumes in a poloidal cross section (Fig. 1). With the recently installed ultra fast transient recorders for data acquisition it is now possible to reduce the time delay between lasers down to 500 ns, and, in addition, the accu-

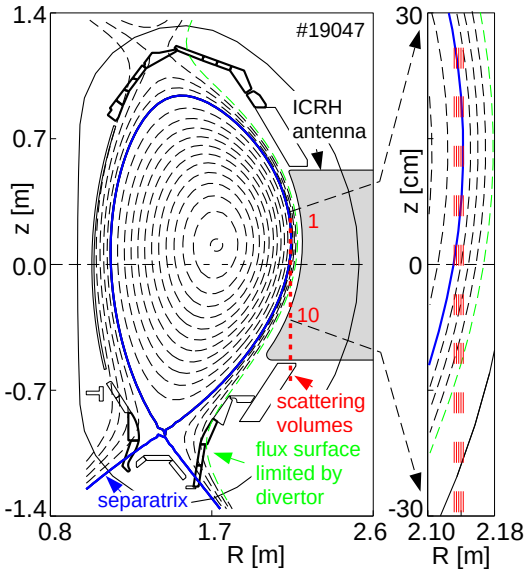

Figure 1: poloidal cross section

racy of the measured data is much increased due to improved background noise treatment [7]. The parameters of the discharges #19046 and #19047, which are investigated mainly in this paper, are: toroidal magnetic field $B_t = -3.0$ T, plasma current $I_p = 800$ kA, safety factor $q_{95} = 7.5$, line-averaged density $\overline{n}_e = 5 \times 10^{19}$ m^{-3}, heating power by neutral beam co-injection $P_{NBI} = 7.8$ MW, elongation $\kappa = 1.82$, upper triangularity $\delta_u = 0.24$, lower triangularity $\delta_l = 0.45$, rather similar to those in [4].

Results

The electron density and temperature values measured locally in the poloidal plane during an 'exposure time' of 2 μs (duration of a laser burst sequence) are presented in the following in the form of contour plots. If the error of measurement is larger than the actual measured value, the data point is set to zero. The radial coordinate in the plots is the major radius R minus the outer most position R_{out} of the separatrix on the low-field side, as determined from magnetic signals.

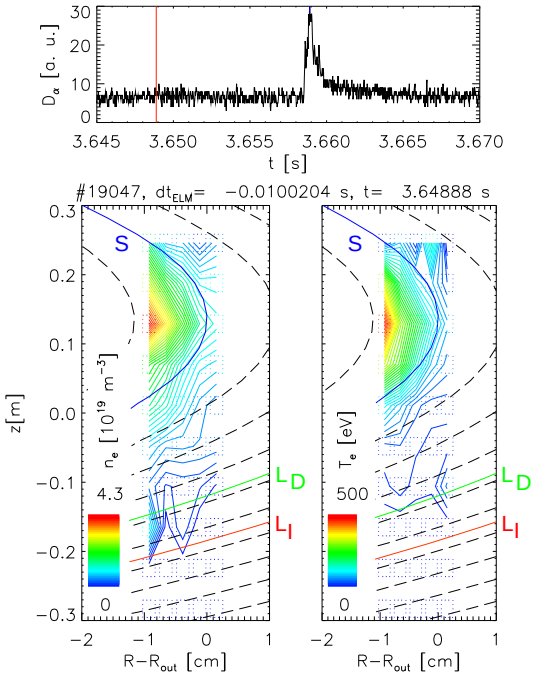

Figure 2: quiescent phase before ELM

A quiescent phase 10 ms before the ELM as marked in the time trace of the D_α-signal (fig. 2) is used to check the accuracy of the determined electron density and temperatures. The error in the spatial position of the flux surfaces, obtained by the equilibrium code CLISTE, is about 5 mm. The deviations between the contours of constant electron density and temperature and the shape of the flux surfaces, as determined by equilibrium reconstruction from magnetic signals, are within the systematic errors of the measured electron densities and temperatures.

At a time of 0.58 ms before the ELM (fig. 3) the contours of constant electron density show local 'blob' structures along a flux surface around the separatrix. These structures are also slightly seen in the electron temperature. The 'blobs' in the electron density are not due to the systematic errors in the measurement of the electron density, which are visible in fig. 2. When these structures are interpreted as field aligned helical structures, the toroidal mode number n can be estimated from the difference of the poloidal angle $\Delta\vartheta$ where these structures occur and the local pitch angle of the magnetic field line. The deduced toroidal mode number for the 'blob' structure before the ELM is $n = 10$. Up to now such 'blobs' have been observed up

to 1.4 ms before the ELM and always at the same spatial position. They are therefore interpreted as locked ELM precursors. In a phase 113 μs after a maximum in the D_α-intensity the difference $\Delta p_e = -290$ Pa between the pedestal pressure and the mean pedestal pressure, which is averaged in time including ELMs, is strongly negative. The electron density and temperature values inside the separatrix constituting the 'holes' are set to zero, because the raw data indicate electron temperatures below 1 eV where reliable electron temperatures and densities can no longer be determined. Maxima are seen in a threefold electron density and a twofold electron temperature structure around and outside the separatrix (fig. 4). The maxima of the structure in the electron temperature do not coincide with the positions of maxima in the threefold structure of the electron density. When these 'blobs' are again interpreted as helical structures, toroidal mode numbers of n = 20, and n = 14 are found for the electron density, and the electron temperature respectively. Particles and energy from the pedestal have obviously been transported to the 'blobs' around the separatrix, leaving 'holes' further inwards. Together with measurements from another discharge (#19807) where the Thomson scattering system was measuring inside the separatrix, the average radial and poloidal diameters of such 'holes' are estimated to be about 6 mm and 8 cm respectively and they are located around 1 cm inside the separatrix in the steep gradient region.

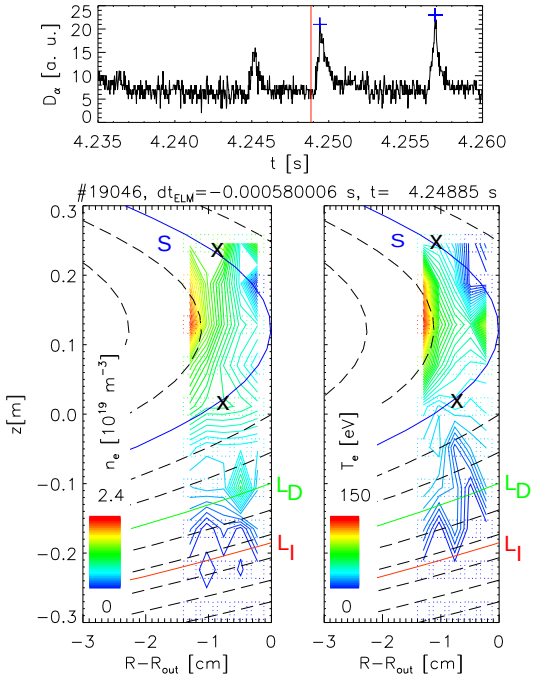

Figure 3: locked ELM precursor

Discussion

Since spirals of the ELM's filaments are observed outside the separatrix on the divertor plates by Thermography [2] apparently a reconnection of the magnetic field lines has taken place and the filaments in the SOL are no longer connected to the main plasma. Interpreting the 'blobs' observed in the SOL as non-rotating vertically elongated filaments a mean radial outward velocity of the filaments between 200 ms^{-1} and 800 ms^{-1} is estimated with [8]. These radial velocities and the typical toroidal and poloidal plasma velocities at the plasma edge of below 10 kms^{-1} are small enough that the 'blob' structures are only neglibly smeared out during the 'exposure time' of 2 μs. The number of independent filaments which exist in the SOL can be estimated by

scaling the number of 'blobs' observed in the SOL by Thomson scattering with the ratios of the poloidal area extending over one poloidal transform and the small area covered by Thomson scattering. This results in about 80 filaments during an ELM. Assuming that the particles confined in the filaments just outside the separatrix are lost to the divertor with ion sound speed during the ELM, lasting for about 1 ms, a particle loss by filaments comparable to the relative global particle loss due to an ELM of some percent is estimated. This observation is in agreement with the results summarized in [9] but in contrast to [1] where only a small number of filaments per ELM is observed, which must be connected to the main plasma to account for the global particle loss of the plasma. A time evolution in the mode numbers of the 'blobs' is found. At times of O(1 ms) before an ELM for co-injected plasmas locked precursors with $n = 9 - 10$ are detected. Up to O(100 μs) after the maximum in the D_α radiation 'blobs' with $n = 14 - 20$ are found. At times of O(1 ms) after the ELM 'blobs' with $n = 8 - 20$ are observed.

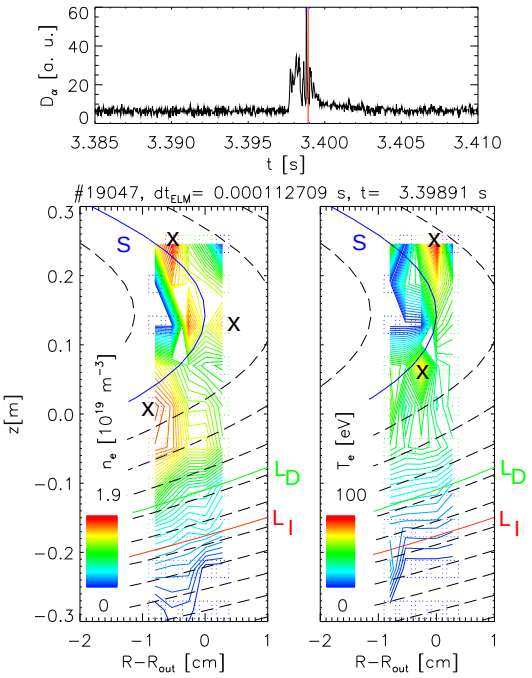

Figure 4: during ELM

References

[1] A. Kirk *et al.*, Plasma Phys. Control. Fusion **47**, 315 (2005)

[2] T. Eich *et al.*, Plasma Phys. Control. Fusion **47**, 815 (2005)

[3] A. Herrmann *et al.*, Plasma Phys. Control. Fusion **46**, 971 (2004)

[4] A. Kirk *et al.*, Plasma Phys. Control. Fusion **47**, 995 (2005)

[5] H. W. Müller *et al.*, Proc. 29th EPS Conf. on Plasma Phys. and Control. Fusion **26B**, O-2.06 (2002)

[6] H. D. Murmann *et al.*, Rev. Sci. Instrum. **63**, 4941 (1992)

[7] B. Kurzan *et al.*, Plasma Phys. Control. Fusion **46**, 299 (2004)

[8] D. A. D'Ippolito *et al.* Phys. Plasmas **9**, 222 (2002)

[9] M. Endler *et al.*, Plasma Phys. Control. Fusion **47**, 219 (2005)